Received: 14 February 2023 | Revised: 6 June 2023 | Accepted: 16 June 2023

IET Nanobiotechnology

DOI: 10.1049/nbt2.12144

ORIGINAL RESEARCH

Natural compound chaetocin induced DNA damage and apoptosis through reactive oxygen species-dependent pathways in A549 lung cancer cells and in vitro evaluations

Qi Zhang[1] | **Feng Ruan**[1] | **Maonan Yang**[2] | **Qinghui Wen**[3]

[1]TCM Teaching and Research Office, Leshan Vocational and Technical College, Leshan, China

[2]Department of Oncology, Leshan Hospital of Traditional Chinese Medicine, Leshan, China

[3]Department of Clinical Laboratory, Dongguan People's Hospital, Dongguan, China

Correspondence

Qinghui Wen, No. 78, Wan Road, Wanjiang District, Dongguan, Guangdong, China.
Email: Qinghui2Wen@hotmail.com

Abstract

There is an urgent need for potential pharmaceutics for lung cancer treatment due to the increased number of lung cancer deaths and the resistance of cancer cells to present therapeutics. The present work aims to discover the anticancer potential of the natural compound chaetocin as a therapeutic for lung cancer treatment. Results showed the significance of chaetocin-induced cell growth inhibition by the expression of G_2/M phase arrest and reactive oxygen species (ROS) dependent apoptosis in A549 lung cancer cells. Results concluded that chaetocin could produce ROS and nuclear damage against A549 lung cancer cells. Interestingly, chaetocin exhibits a significant level of CD47 that down-regulates the expression of CD47 at mRNA levels. PBMC biocompatibility study revealed that chaetocin is non-toxic to normal cells. Overall, experimental results suggested that chaetocin induces A549 cell apoptosis, by causing ROS and nuclear damage activation pathways. In the future, chaetocin might be an effective bio-safe anticancer agent for lung cancer treatments.

KEYWORDS

biochemistry, biomedical materials, cancer, lung

1 | INTRODUCTION

Lung carcinoma is a frequently detected life-threatening disease in the world. Lung carcinoma is one of the cruelest life-changing illnesses in human society. Exact disease identification is vital for effective cancer therapy; every carcinoma needs a specific treatment strategy [1–4]. The usual treatments like surgery, radiotherapy, chemotherapy, hormonal treatments, and biological therapies are highly toxic and expensive. The correct selection of therapeutics and treatment protocols is essential to achieve an effective result [5–7]. Synthetic anticancer drugs cause adverse side effects on normal cells and organs. High mutation rates of lung cancer cells resulted in unsatisfactory effects of drugs. Therefore, novel and biosafe anticancer drugs are the current need for lung cancer treatment [6–8]. Reactive oxygen species (ROS) has associated with many biological mechanisms, including cell proliferation, toxicity, and nuclear damage through interaction with cell signalling pathways [9–12]. Recently, a variety of scientific evidence has shown that ROS accumulation is closely related to atherosclerosis, diabetes mellitus, and tumours [13–15]. In cancer, an increase in ROS accumulation apart from normal counterparts leads to cell death. Cancer cells' production of ROS is highly vulnerable. Redox-targeted drugs might be the most efficacious in cancer treatments [13, 16, 17]. On the other hand, immune inhibitors and DNA-damaging anticancer agents are new checkpoints in cancer therapy [18, 19]. Contrarily, plant-derived compounds are a promising resource for new anticancer drug discovery. About 50% of FDA-approved anticancer drugs are of natural materials [20–23]. The exploration of potential anticancer agents from natural resources seems to be a charming technique. Chaetocin is a fungal metabolite produced by Chaetomium and has an excellent inhibitory effect against different types of cancer cells. Recent research outcomes proved that the anticancer potential of chaetocin depends on ROS accumulation [24–27]. Antiproliferative effects of chaetocin in cancer

cells are reported. But the cellular mechanism of the anticancer effect is unclear [28, 29]. In the present work, we investigated the antiproliferative and apoptotic mechanism of chaetocin in A549 lung cancer cells. In addition, the immune pathways CD47 expression, DNA damage, and mitochondrial membrane potential (MMP) were examined via different staining techniques. The outcome results of this research work highlighted chaetocin as a biosafe and effective chemotherapeutic agent for lung cancer treatment.

2 | MATERIALS AND METHODS

2.1 | Chemicals

Chaetocin, Dulbecco's modified eagles' medium (DMEM), JC-1 stain, Ethidium Bromide (EB), N-acetyl-L-cysteine (NAC), Dichloro-dihydro-fluorescein diacetate (DCFH-DA), Propidium iodide (PI), Acridine Orange (AO), Annexin V-FITC, 4′,6-diamidino-2 phenylindole (DAPI), and Hoechst 33,342 were purchased from Sigma Aldrich, USA. Primary antibodies against caspase-3 were purchased from Cell Signalling Technology (Beverly, USA). Foetal bovine serum (FBS), dimethyl sulfoxide (DMSO), antibiotic solutions (Penicillin and Streptomycin), and dimethylformamide (DMF) were purchased from TaKaRa Biomedical Technology, China.

2.2 | Cell culture

A549 cell line was obtained from the Culture Collection of the Chinese Academy of Science (Shanghai, China). A549 lung cancer cells were pre-cultured in DMEM with 10 μg/mL streptomycin, 10% foetal bovine serum, and 100 units/mL penicillin. The incubation period was continued under a humidified atmospheric environment at 37°C with 5% of CO2 flow.

2.3 | Cell viability assay

The cytotoxic effect of chaetocin versus A549 cells was examined by using a cell counting kit-8 (CCK-8) assay. Cells were seeded in a 96-well plate and maintained under suitable conditions overnight to grow. After the overnight culture, chaetocin at different concentrations (20–100 nM) was loaded and again incubated for another 24 h. Treated cells were washed with PBS solution for removal of excess cell medium. Further, 10 μL of CCK-8 solution was added into each well and continued 4 h incubation. The optimum density of the culture medium was recorded by using a Flash multimode reader (Thermo Fisher Scientific, USA) at the 450 nm range.

2.4 | Assessment of colony-forming units

1000 cells/well of A549 cells seeded into 12-well plates. Chaetocin at various concentrations (0.626, 1.25, and 2.5 nM) was added into a cell containing wells. The cell seeded plate was incubated at 37°C, and inhibition was measured in different time durations. Before the microscopic observation and imaging, cells were fixed in glass slides using ice-cold methanol and stained with 0.1% crystal violet solution. The total number of colonies was calculated from images obtained by the Epson scanner instrument.

2.5 | Real-time cell analysis

The proliferation rate of A549 cells was systematically evaluated by the xCELLigence system (Germany). Briefly, A549 lung cancer cells were seeded in an E-plate with 100 μL of media and incubated overnight at 37°C. After that, the incubated cells were treated with Chaetocin (12.5, 25, and 50 nM) in different doses. The enhancement of impedance was measured according to the guidelines of the manufacturer protocols. The value of impedance increases as the cells proliferate.

2.6 | Analysis of cell cycle

Chaetocin-induced cell cycle arrest was examined by using FACSCanto II flow cytometry with the Propidium iodide (PI) staining method. A549 cells were treated with 100 and 250 nM concentrations. Then, the chaetocin treatment cells were washed with 66% of cold ethanol solution at 4°C for fixation, and the ethanol removal cells were stained with PI stain.

2.7 | Analysis of apoptosis

The apoptotic percentage of chaetocin-treated A549 cells was quantified by Flow cytometry with Annexin V-FITC/PI staining assay. After the chaetocin exposure, the attached cells were washed with PBS. Further cells were stained by 5 μL of PI and Annexin V-FITC stains with 500 μL of binding buffer solution. Cells were kept for 15 min under the dark condition at room temperature. Quantification was carried out by using FACSCanto II flow cytometry (BD Biosciences). The Annexin V-FITC stain-emitting cells were considered apoptotic cells. The morphology of chaetocin-treated A549 cells was assessed by AO/Br dual staining under a fluorescence microscope [11]. The commercial anticancer drug 5-fluorouracil was considered a positive control. The percentage of apoptotic cells was quantified through the red/green fluorescence intensity of treated cells.

2.8 | Measurement of mitochondrial damage

Damage to mitochondrial membrane potential (MMP) of A549 cells was evaluated by JC-1 staining kit (Nanjing KeyGen Biotech, China.) according to Prabhu et. al, 2019 [11] manufacturer's protocol. Cells were treated with various doses of chaetocin (12.5, 25, and 50 nM) and stained with JC-1 (1 μg/mL–1) for 20 min at 37°C. After staining, the excess stain was

washed by PBS. Fluorescence intensity was recorded by using FACSCanto II flow cytometry. The loss of MMP was quantified from the fluorescence intensity of treated cells. While cells exposed to JC-1 aggregates and red fluorescence which considered healthy cells. Finally, fluorescence cell images were captured in an Olympus fluorescence microscope.

2.9 | Assessment of ROS generation

Chaetocin-induced reactive oxygen species (ROS) were examined by 2′,7′- dichlorofluorescein diacetate (DCFH-DA) fluorescence assay [12]. A549 cells were incubated with 10 μM of DCFH-DA fluorescent probe at 37°C for 30 min. Cells were treated with different concentrations of chaetocin (12.5, 25, and 50 nM). Before flow cytometry, fluorescence measurement cells were washed with serum-free media and resuspended in 500 μL of PBS solution. Morphological changes of chaetocin-treated A549 cells were observed under a fluorescence microscope. Images were captured at 20x magnification.

2.10 | Assessment of nuclear damage

Nuclear damage of A549 cells induced by chaetocin was evaluated by Hoechst staining according to the previous method [12]. Cells are treated with chaetocin 50 nM concentration and subjected to 1 mg/mL Hoechst staining for about 15 min. After treatment, cells were washed with phosphate buffer saline. The fluorescence intensity and nuclear damages were visualised under a fluorescence microscope at 365/420 nm (excitation/emission) wavelengths. Commercial anticancer drug 5-fluorouracil is used as a positive control. The percentage of live/dead cells was quantified from more than a hundred treated cells.

2.11 | Western blot analysis

Followed by the chaetocin treatment, A549 lung cancer cells lysed in RIPA buffer solution containing protease and phosphatase inhibitors. The concentrations of every protein sample were measured by the Pierce BCA protein assay kit (Thermo Fisher Scientific, USA). Total cellular proteins were separated by SDS-PAGE and transferred into PVDF membranes. After the blocking of 5% non-fat dry milk, membranes were probed with primary antibodies at 4°C for 12 h. Finally, membranes were washed with PBST and incubated with a horseradish peroxidase-conjugated secondary antibody. The results were detected using enhanced chemiluminescence.

2.12 | Cell migration assay

Skin fibroblast cells L929 and A549 lung cancer cells were seeded into separate 24 well plates with 2 mL of DME medium and cultured for 24 h at 37°C [30]. When the cells proliferate more than 90%, a 100 μL pipette tip was used to wound scratching of L929 and A549 cells in a 24-well plate. The cell was treated with a 50 nM concentration of chaetocin and cultured for another 12 h. Wells without the addition of chaetocin is considered a negative control. Cell proliferation and migration were observed under an inverted phase contrast microscope. The percentage of wound closure and invasion of L929 and A549 cells was quantified at 12 h. All the wound scratch assays were carried out in triplicates. The migration rate of chaetocin-treated cells was measured by ImageJ 1.4 software.

$$\text{Wound closure } \% = \frac{\text{A0} - \text{At}}{\text{At}} \times 100$$

where A0 is the average area of wound closure at initial time (0 h), and At is the average area of the wound closure after treatment.

2.13 | In vitro biocompatibility study

Cytotoxicity of chaetocin was examined by MTT assay against peripheral blood mononuclear cells (PBMC) as an in vitro model [12]. PBMC cells were treated with different concentrations of chaetocin (20–100 nM) at 37°C for 24 h. A 250 nM of hydrogen peroxide was considered a positive control for comparison. The cytotoxic effect was quantified from the number of viable cells.

2.14 | Statistical analysis

All the cell culture tests were performed as triplicates. All results are shown as ± SD mean values. The significant difference in results was analysed by GraphPad Prism7.00 (GraphPad Software Inc, US) $^*p < 0.05$ is statistically significant.

3 | RESULTS

3.1 | Chaetocin suppressed A549 cell growth and G2/M expression arrest

Chaetocin has a significant cytotoxic effect on A549 cells. After treatment with different doses of chaetocin for 24 h, the cell counting kit-8 results showed significant cell inhibition depending on the dose of chaetocin. The IC_{50} values are between 56.02 ± 1.2 nM (Figure 7c). Real-time analysis exhibits a dose-dependent manner inhibition of normalised cell index in chaetocin-treated A549 cells (Figure 1b), and it is indicating the controlled cell proliferation of A549 cells by chaetocin. The results of the colony-forming assay exhibit a decreased size and numbers in A549 cells. Interestingly, results demonstrated that chaetocin effectively suppressed A549 cell growth. Cell cycle arrest and distribution were examined by the flow cytometry method (Figure 2a–c). Whether chaetocin-treated cells showed a progressive level of cell cycle arrest, after 12 h post-exposure. The total population of A549 cells at the G2/M phase substantially increased in the higher dose (Figure 2d). This

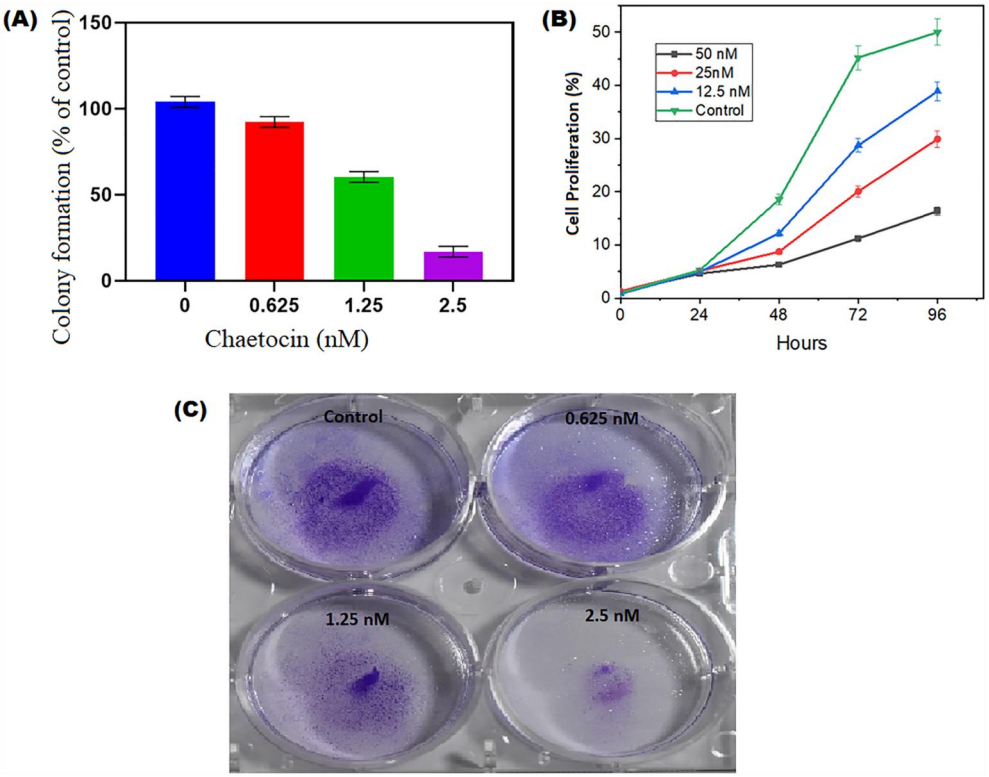

FIGURE 1 (a) Chaetocin inhibits A549 cell colony forming unit at different concentrations (b) Real time cell analysis of A549 cells inhibition after chaetocin treatment at different days and different concentrations. (c) A549 cells treated with different concentration of chaetocin (0.625, 1.25 and 2.5 nM) and colony formation. Results presented here are representative of three independent experiments. Results in (a and b) are shown as mean ± SD of three independent experiments. $^*P < 0.01$ versus control group.

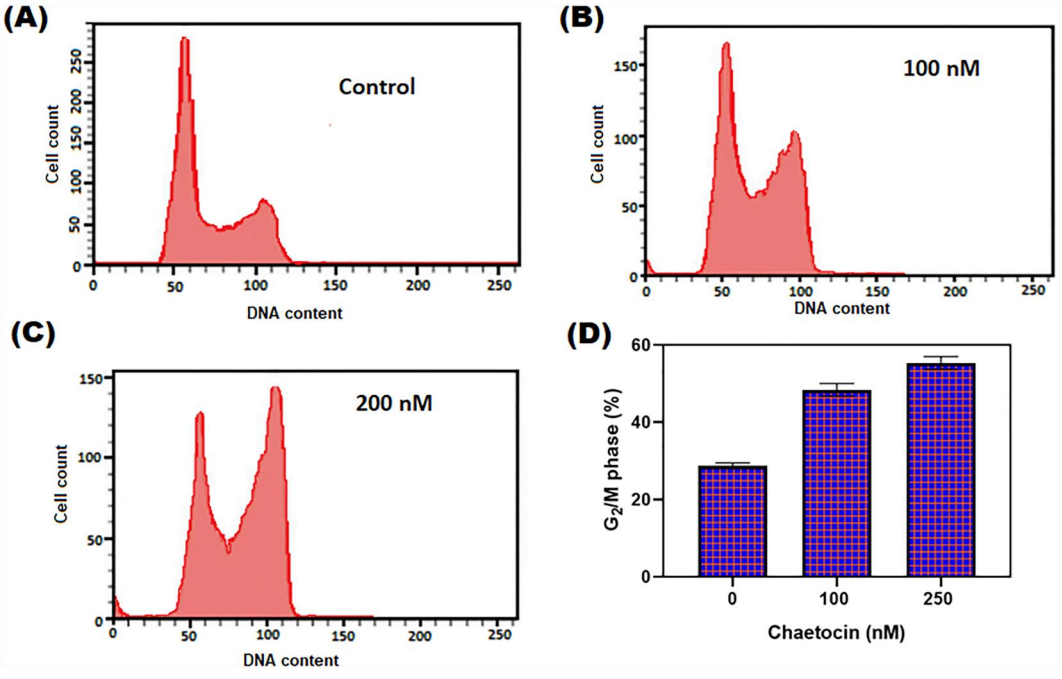

FIGURE 2 (a–c) The cell cycle distribution of A5549 cells 12 h with chaetocin treatment at different doses (100 and 200 nM) by PI-staining (d) Depression of G_2/M phase with chaetocin treatment at various concentrations. Results were shown as mean ± SD of triplicate experiments. $^*p < 0.05$ versus control cells.

indicates that chaetocin effectively inhibits the A549 cell proliferation by the G2/M phase suppressed mechanism.

3.2 | Chaetocin-induced apoptosis by mitochondrial membrane potential damage

In JC-1 staining, after chaetocin treatment, A549 cells exhibited increased mitochondrial membrane potential (MMP) damage and apoptotic cell populations. The apoptotic population was multiplied based on increased concentration and duration of treatment. The MMP damage pathway is a crucial action for apoptosis [9]. Chaetocin-induced caspase-3 and protein cleavage lead to the cell death process in A549 cells. The decrease of membrane integrity of mitochondrial indicates apoptosis. Figure 3 shows the damage to mitochondrial membrane integrity in A549 cells after chaetocin treatment. In quantification, more than 40% of cells were exposed to mitochondrial damage in a dose-dependent manner. In higher concentrations (50 nM), chaetocin significantly exposed MMP damage at 36 h.

3.3 | Accumulation of ROS in chaetocin-induced A549 cell

Chaetocin induces an apoptotic effect through ROS accumulation in A549 cells after treatment. The fluorescent intensity of DCFH/DA was increased after chaetocin treatment, which indicates the ROS generation in cells. Results revealed that Chaetocin-induced apoptosis in cells depends on the overproduction ROS of an intracellular region. In control and chaetocin (12.5 nM)-treated groups, the basal level of DCF-sensitive ROS production was not detectable in the initial period. In the treatment with chaetocin (25 and 50 nM) concentrations, a significant level of ROS generation appeared at early 30 min. When compared to the control cells, chaetocin-treated A549 cells showed a razor-sharp increase in intracellular ROS accumulation (Figure 4). The fluorescence microscopic images of chaetocin-treated cells showed radiant green fluorescence. Chaetocin-induced ROS generation has a close relationship with apoptosis and mitochondrial dysfunction mechanisms. At the apoptosis-leading 50 nM concentration, chaetocin generates a significant amount of intracellular ROS and free radicals within 30 min of post-exposure. The free radical formation was accelerating cell death by damaging cellular DNA, lipids, and mitochondrial membranes.

3.4 | Chaetocin-induced apoptosis in A549 cells

The apoptosis mechanism of chaetocin-treated cell morphology was investigated via AO/Br dual staining assay. The treatment of chaetocin caused structural and nuclear changes in A549 cells

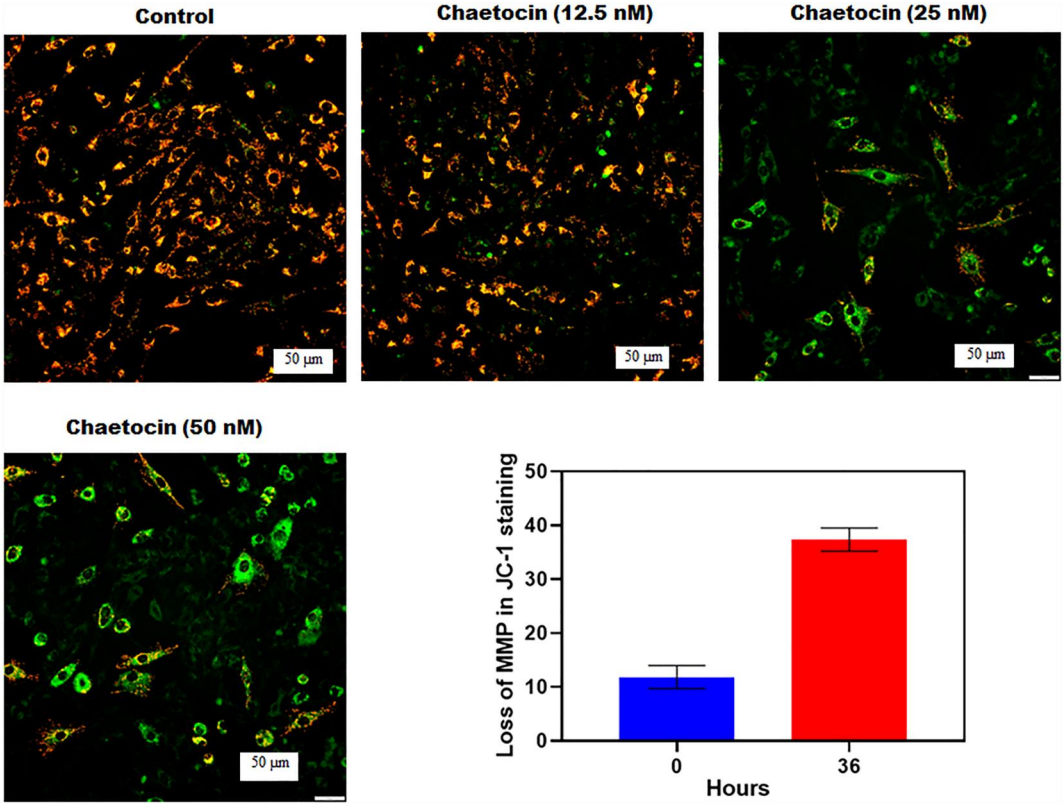

FIGURE 3 The bar graph represented the loss of mitochondrial membrane potential (MMP) after treatment of chaetocin at the different times recorded by flow cytometry (JC-1 staining). The fluorescence microscopic images indicate the morphological changes of A549 cells after chaetocin treatment at 20x magnification.

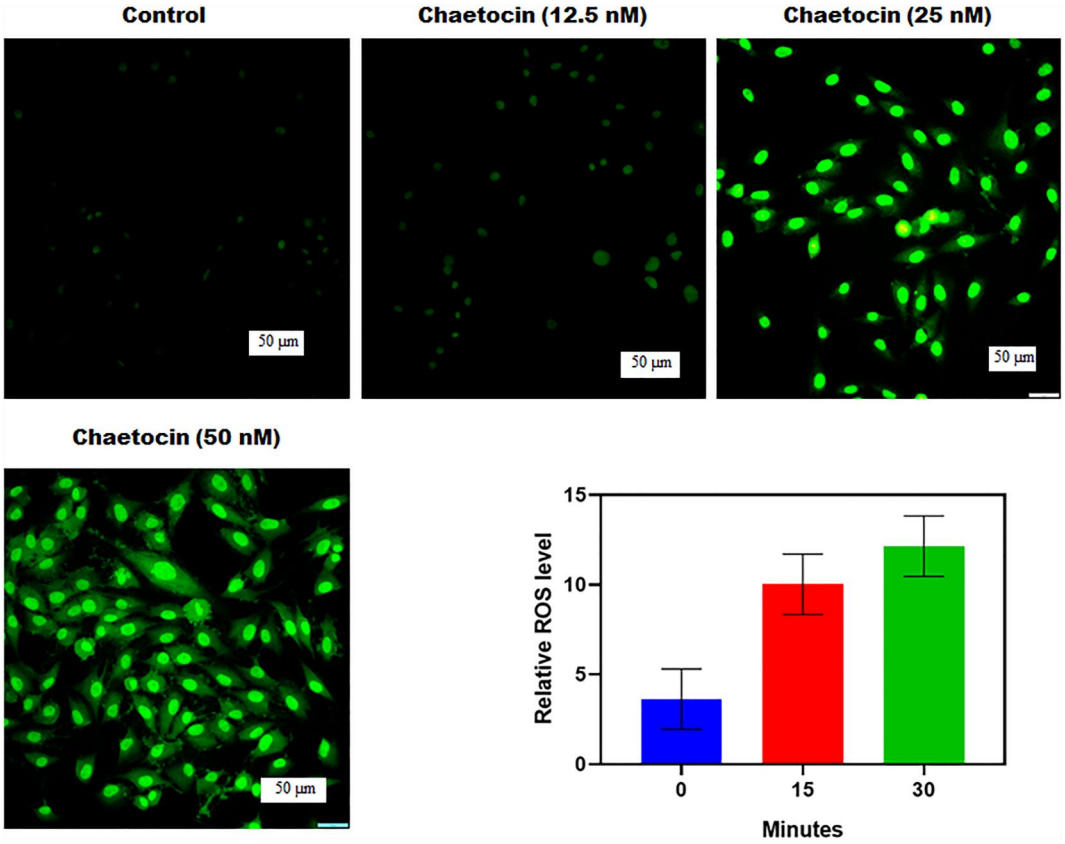

FIGURE 4 Chaetocin leading apoptosis in A549 cells is associated with ROS generation. The bar graph indicates the generation of ROS after chaetocin exposure at different periods. Fluorescence microscopic images represent the structural and cytological changes of treated cells in 50 µm scale at 20x magnification. Results were shown as mean ± SD of triplicate experiments. *$p < 0.01$ versus control group.

when compared to control cells. The main structural changes were found in A549 cells after treatment. Apoptosis was evaluated through AO/EB dual staining assay (Figure 5). In AO/EB dual staining assay, live cells turn to emit green fluorescence and can distinguish from apoptotic cells. After chaetocin treatment, a significant amount of live cell reduction was detected in chaetocin-treated groups. Red cells were only observed in the chaetocin and 5-fluorouracil treatment. In the flow cytometry technique, Annexin V-FITC and PI staining results revealed the apoptotic effect of chaetocin that could stretch into A549 cells after treatment. A very similar IC_{50} value of 54.3 ± 1.5 nM was recorded in the CC8 kit cell viability assay (Figure 7c). The percentage of apoptotic cells was increased after a 36 h post-exposure. These experimental results indicate that A549 cell death after chaetocin treatment occurred through the apoptosis mechanism.

3.5 | Nuclear damage Hoechst staining

The apoptotic mechanism plays a promising role in changes in cellular morphology and biochemicals [31, 32]. The cytotoxic effect of chaetocin related to nuclear changes was assessed by Hoechst 33,342 staining technique. The quantitative percentage of normal/abnormal cell nuclei of 5-fluorouracil and chaetocin-treated A549 cells showed 56.12 ± 0.24 and 72.35 ± 0.14% of abnormal nuclei. Control cells exhibited only 4.1 ± 0.15%. Microscopic image control revealed the availability of normal cell nuclei with less blue fluorescence. In this case, chaetocin-treated cells exhibit bright blue fluorescent with cytomorphological changes such as chromatin fragmentation, irregularity of nuclear structure, binucleation, and shrinkage of nuclei (Figure 6). The intra-cellular changes illustrate the fact that apoptotic mediated cell death. The results of Hoechst's assay suggest the death of A549 cells reflected by the cytotoxic effect of chaetocin.

3.6 | Chaetocin-mediated CD47 expression decreases in A549 cells

CD47 is a leading key immune checkpoint in cancer treatments [33, 34]. The western blot assay showed that chaetocin suppresses the CD47 expression at the mRNA level. It inhibits the total CD47 protein expression and CD47 membrane protein in A549 cells (Figure 7a). High level of CD47 expression on the cancer cell surface enables the macrophages' immune surveillance. Results revealed that chaetocin pre-treated A549 cells showed enhanced phagocytosis. It is indicating the reduction of CD47 expression in A549 cells, as well as the ROS

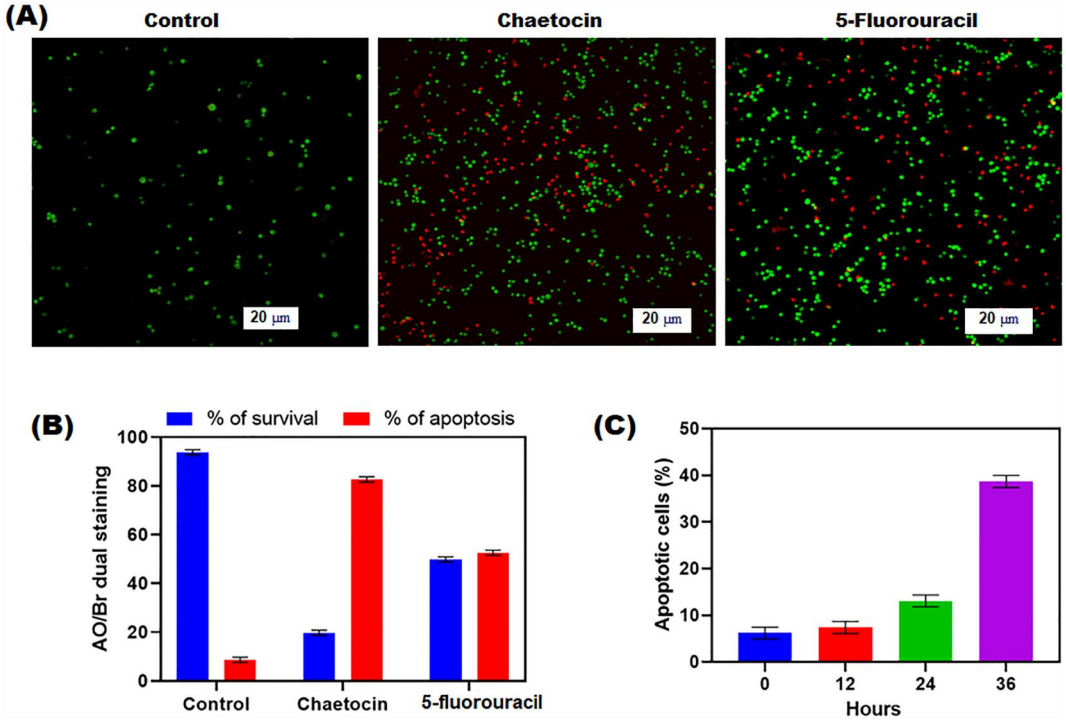

FIGURE 5 Apoptotic effect of chaetocin-treated A549 cells by AO/EB dual staining. Percentage of live/dead cell populations assessed by Annexin V-FITC/PI staining in flow cytometry. (a) Fluorescence microscopic images indicate the morphological changes of chaetocin-treated A549 cells in 20 µm scale at 20x magnification. (b) Precentage of live and apoptotic cells after the treatment of chaetocin and 5-fluorouracil. (c) The percentage of apoptotic cells after treatment of chaeticin at differnet time intervals (0, 12, 24, 36 h). Data are expressed as mean ± SD of triplicate assays. $*p < 0.001$ Control versus drug treated groups.

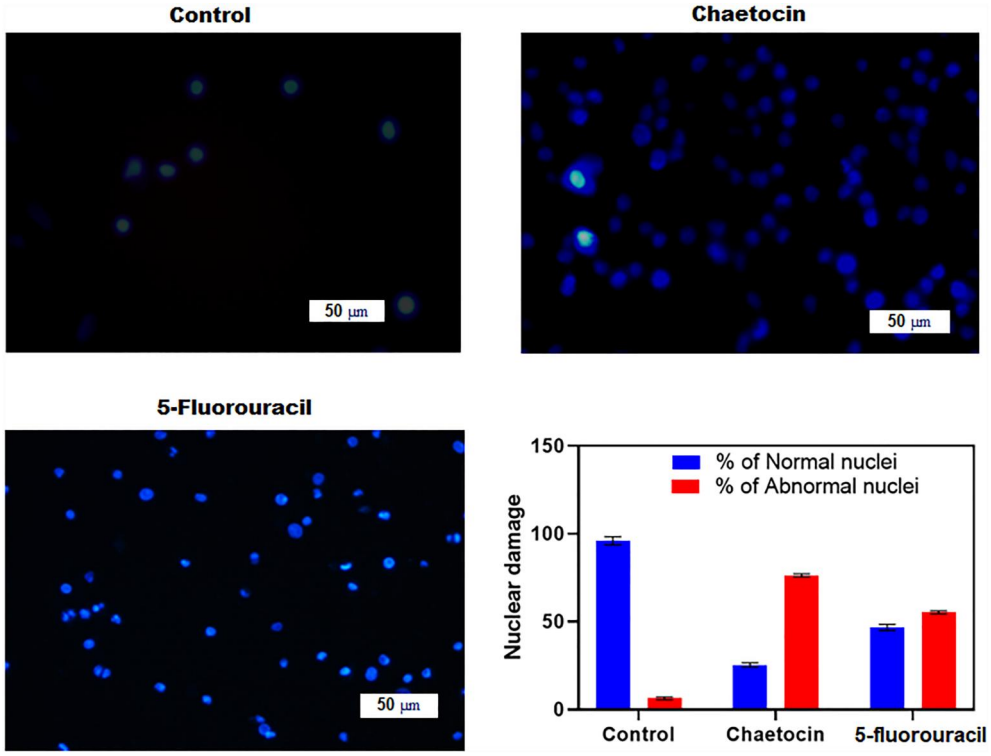

FIGURE 6 Chaetocin induced nuclear damage was evaluated by Hoechst 33,342 staining. Fluorescence microscopic images illustrating nuclear fragmentation and deformities at 20x magnification. The bar graph represents the percentage of normal and abnormal nuclei in the treated groups. Quantitative results for the number of apoptotic cells per 100 cells in total. $*p < 0.05$ denotes the statistical significance between the control and treated group with respect to normal and abnormal nuclei. Cellular images were captured in 50 µm scale at 20X magnification.

generation potential of chaetocin involved in the down-regulation mechanism of CD47 protein expression at mRNA transcript levels. These western blot results indicate that chaetocin can effectively decrease CD47 expression at mRNA levels in A549 cells and stimulates phagocytosis (Figure 7b).

3.7 | Biocompatibility

The in vitro biocompatibility of chaetocin was examined against human peripheral blood monoclonal cells (PBMC) by trypan blue exclusion assay. The results revealed that no significant level of cytotoxicity was observed in treated cells. The highest concentration of 400 and 500 nM shows only 3% of cytotoxicity in post-treatment. Lower concentrations are very similar to the control group. In this case, positive control H_2O_2 treated cells showed a significant amount of cell death after treatment, with only 24 ± 0.12% viable cells available at 250 nM concentration (Figure 7d). The result suggested that chaetocin is more biosafe for human normal blood cells and a more suitable drug for cancer therapy.

3.8 | Assessment of migration and invasion of L929 and A549 cells

The migration of cancer cells is a main cause of increased cancer deaths [35, 36]. The in vitro wound scratch tests were utilised to examine the migration and invasion of L929 cells and A549 cells against chaetocin. In the control group, chaetocin had no negative impact on the migration of L929 cells. Chaetocin treatment enhances the cell proliferation and migration rate of the L929 cells within 12 h. The number of cells and migration rate increased in dose-dependent manner. Interestingly, A549 cells showed a significant level of cell inhibition and migration reduction after treatment with chaetocin. Compared with a control group, a 50 nM concentration of chaetocin showed a great inhibitory effect on the A549 cell (Figure 8). This result suggests that chaetocin effectively controls the migration of lung cancer cells. It might be an effective plant-derived drug for lung cancer treatment.

4 | DISCUSSION

Novel therapeutic agents for lung cancer are an urgent need, and biomaterials are prominent resources for new and effective drug discovery. In the present study, by the evaluations, fungal metabolite chaetocin not only induces cell death based on cell cycle arrest. It also downregulates or suppressed the CD47 expression at mRNA levels and the accompanying phagocytosis by macrophages in A549 lung cancer cells. This investigation results underline the importance of chaetocin in lung cancer control. The basal ROS accumulation level is higher than normal counterparts and more vulnerable to A549 cells [17, 37]. This study reports a significant level of ROS increases and mitochondrial membrane damage-induced cell apoptosis. Blocking ROS production and resistance to cancer is a major

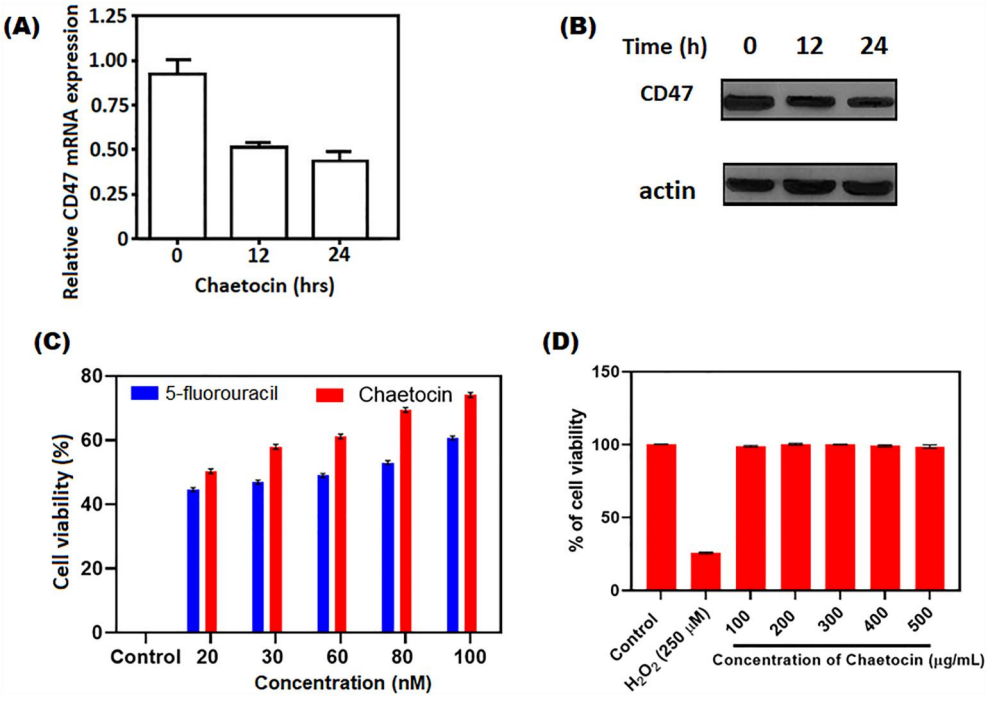

FIGURE 7 Chaetocin mediated the decrease of CD47 expression and enhancement of phagocytosis of macrophages in A549 cells. (a) The expression of CD47 was recorded by qPCR on A549 cells after chaetocin at various time intervals (b) Expression of total CD47 protein at different periods by western blot technique. (c) Cytotoxicity of chaetocin against A549 cells at different concentrations using CCK8 cell viability assay (d) Cytotoxicity of chaetocin against PBMC cells using MTT assay $*p < 0.05$ indicates the statistical significance between control and treated groups.

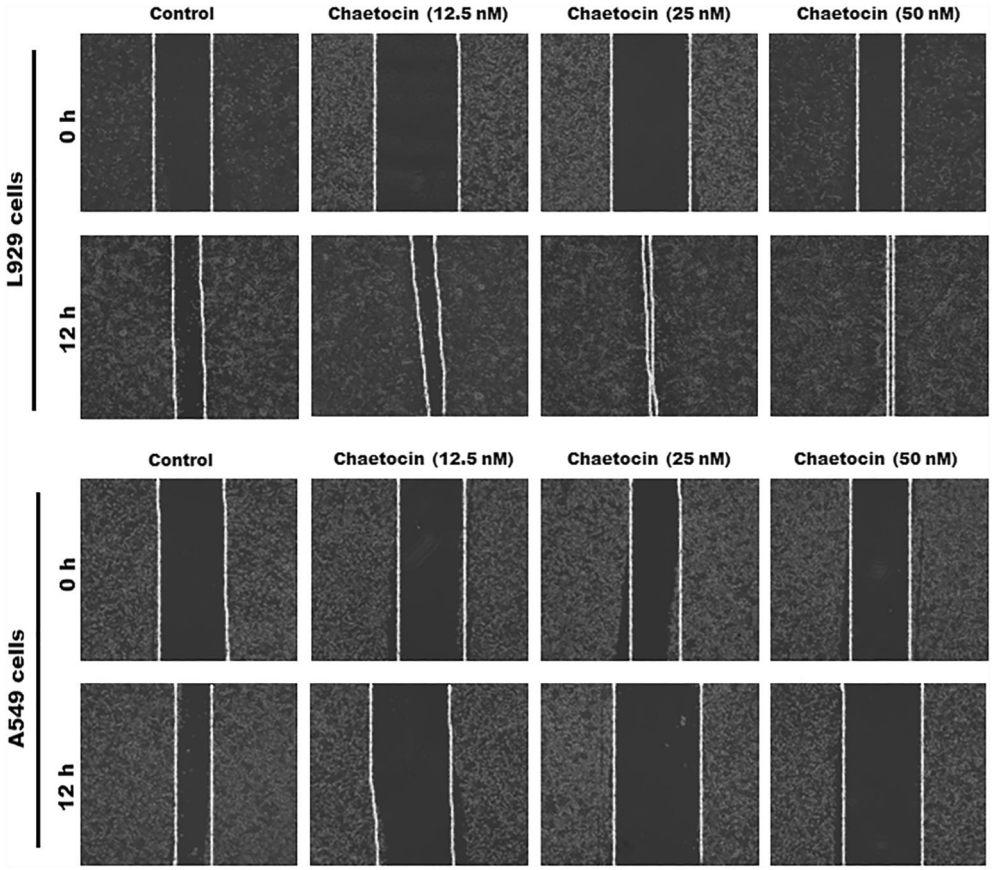

FIGURE 8 Wound healing potential of chaetocin against L929 cells and A549 cells; phase contrast microscopic images indicates the migration ability of A549 and L929 cells after the treatment of chaetocin.

abrogation of the cytotoxic effects of anticancer drugs. Interestingly, chaetocin induces mitochondrial membrane and DNA damage-mediated apoptosis. It induces morphological changes, including nuclear dividing and fragmentations, that might be associated with autophagy. Collectively, experimental results confirmed that chaetocin can destroy cancer cells by the induction of necrotic cell death. The results of JC-staining (MMP) and AO/EB apoptosis assay exhibit quite promising effects against A549 cells. In this regard, the damage of mitochondrial membrane potential and intracellular ROS by chaetocin inhibits the thioredoxin reductase enzymes mediated cell necrosis [27, 28]. In Hoechst staining, the chaetocin treatment effectively damages the nuclear region of A549 cells and leads to apoptosis with nuclear fragmentation and binucleation mechanism. Another side chaetocin effectively reduced the CD47 expression at the mRNA level via ROS accumulation. The downregulation of CD47 expression by chaetocin in A549 cells exhibits additional evidence in cancer cell death pathways. The cell migration and invasion study revealed that chaetocin significantly affects cell migration in A549 cells within 12 h. In this case, chaetocin treated with L929 cells showed a higher level of cell migration and cell density compared with A549 cells. After the 12 h treatment, chaetocin exhibits 72% of wound closure at the 50 nM concentration (Figure 9). On the contrary, A549 lung cancer cell showed a significant level of inhibition in cell migration and wound closure at 50 nM of chaetocin treatment. The wound scratch assay suggested that chaetocin can inhibit the multiplication and transport of cancer cells. Further, the PBMC in vitro biosafety evaluation confirmed that chaetocin is a nontoxic agent for normal cells until 500 nM higher concentration. The overall in vitro cytotoxicity and biosafety evaluations concluded that chaetocin is an effective natural anticancer therapy for lung cancer treatment.

5 | CONCLUSION

The present study highlights the cytotoxic potential of chaetocin on A549 cells. The authors also suggested the reduction of CD47 expression and nuclear DNA damage of A549 cells. In addition, ROS and mitochondrial membrane potential damage is the major leading factor of A549 cell apoptosis. Our research findings confirmed the anticancer effect of chaetocin in lung cancer with multi-dimensions. Biocompatibility evaluation confirmed that chaetocin is a more suitable drug for human cancer treatment. The treatment of chaetocin effectively reduced the density and migration rate of the A549 cell. This study demonstrates that chaetocin is a safe and effective drug for lung cancer treatment.

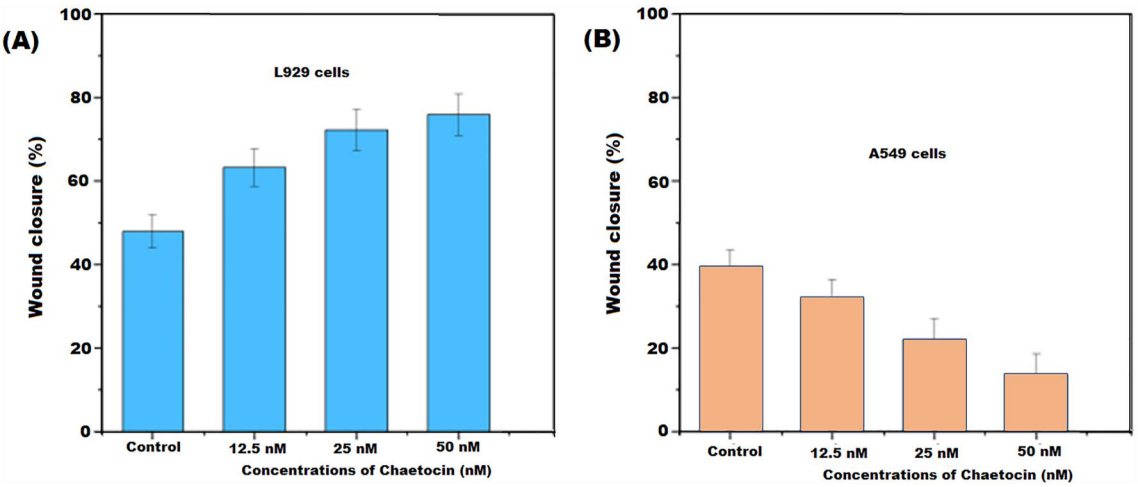

FIGURE 9 The bar diagram expressed the percentage of wound closure after the treatment of chaetocin at 24 h. (a) Percentage of wound closure against L929 cells at diffetent concentration of chaetocin. (b) Percentage of wound closure against A549 lung cells at different cincentration of chaetocin in 50 μm scale. Results are the means of three measurements ($*p < 0.05$).

AUTHOR CONTRIBUTION

All the authors have equal contribution to this study.

CONFLICT OF INTEREST STATEMENT

All the authors declared no conflicts of interest.

DATA AVAILABILITY STATEMENT

The original data were included in the presented article, and further inquiries can be directed to the corresponding author.

ORCID

Qinghui Wen https://orcid.org/0000-0002-4217-6923

REFERENCES

1. Elshami, M., et al.: Current situation and future directions of lung cancer risk factor awareness in Palestine: a cross-sectional study. BMJ Open 13(1), e061110 (2023). https://doi.org/10.1136/bmjopen-2022-061110
2. Tan, P., et al.: Risk factors for refractory immune checkpoint inhibitor-related pneumonitis in patients with lung cancer. J. Immunother. 46(2), 10–1097 (2023). https://doi.org/10.1097/cji.0000000000000451
3. Lucena, C.M., et al.: Integral mediastinal staging in patients with non-small cell lung cancer and risk factors for occult N_2 disease. Respir. Med. 208, 107132 (2023). https://doi.org/10.1016/j.rmed.2023.107132
4. Siegel, R.L., et al.: Cancer statistics, 2023. CA A Cancer J. Clin. 73(1), 17–48 (2023). https://doi.org/10.3322/caac.21763
5. Castellano-Hinojosa, A., et al.: Anticancer drugs in wastewater and natural environments: a review on their occurrence, environmental persistence, treatment, and ecological risks. J. Hazard Mater. 447, 130818 (2023). https://doi.org/10.1016/j.jhazmat.2023.130818
6. Motyka, S., et al.: Podophyllotoxin and its derivatives: potential anticancer agents of natural origin in cancer chemotherapy. Biomed. Pharmacother. 158, 114145 (2023). https://doi.org/10.1016/j.biopha.2022.114145
7. Patel, V.K., et al.: Multi-targeted HDAC inhibitors as anticancer agents: current sta-tus and future prospective. Curr. Med. Chem. 30(24), 2762–2795 (2023). https://doi.org/10.2174/0929867329666220922105615
8. Prabhu, R., Suganthy, N.: Investigation of pesticidal and anti-biofilm potential of Calotropis gigantea latex encapsulated zeolitic imidazole nano frameworks. J. Inorg. Organomet. Polym. Mater., 1–10 (2022)
9. Prabhu, R., Suganthy, N.: Anticancer, antibiofilm and antimicrobial activity of fucoidan loaded zeolitic imidazole framework fabricated by one - pot synthesis method. Appl. Nanosci., 1–19 (2021)
10. Prabhu, R., Pugazhendhi, A., Suganthy, N.: One-pot fabrication of multi-functional catechin@ZIF-L nanocomposite assessment of antibiofilm, larvicidal and photocatalytic activities. J. Photochem. Photobiol. B Biol. 203, 111774 (2020). https://doi.org/10.1016/j.jphotobiol.2019.111774
11. Prabhu, R., et al.: Ecofriendly one pot fabrication of methyl gallate@-ZIF-L nanoscale hybrid as pH responsive drug delivery system for lung cancer therapy. Process Biochem. 84, 39–52 (2019). https://doi.org/10.1016/j.procbio.2019.06.015
12. Raju, P., et al.: Fabrication of pH responsive FU@ Eu-MOF nanoscale metal organic frameworks for lung cancer therapy. J. Drug Deliv. Sci. Technol. 70, 103223 (2022). https://doi.org/10.1016/j.jddst.2022.103223
13. Naik, J., David, M.: ROS mediated apoptosis and cell cycle arrest in human lung adenocarcinoma cell line by silver nanoparticles synthesized using Swietenia macrophylla seed extract. J. Drug Deliv. Sci. Technol. 80, 104084 (2023). https://doi.org/10.1016/j.jddst.2022.104084
14. Schlormann, W., et al.: Potential role of ROS in butyrate-and dietary fiber-mediated growth inhibition and modulation of cell cycle-apoptosis- and antioxidant-relevant proteins in LT97 colon adenoma and HT29 colon carcinoma cells. Cancers 15(2), 440 (2023). https://doi.org/10.3390/cancers15020440
15. Chuang, T.C., et al.: Baicalein induces G2/M cell cycle arrest associated with ROS generation and CHK2 activation in highly invasive human ovarian cancer cells. Molecules 28(3), 1039 (2023). https://doi.org/10.3390/molecules28031039
16. Lin, C.L., et al.: Plumbagin induces the apoptosis of drug-resistant oral cancer in vitro and in vivo through ROS-mediated endoplasmic reticulum stress and mitochondrial dysfunction. Phytomedicine 111, 154655 (2023). https://doi.org/10.1016/j.phymed.2023.154655
17. Yang, H.L., et al.: In vitro and in vivo anti-tumor activity of Antrodia salmonea against twist-overexpressing HNSCC cells: induction of ROS-mediated autophagic and apoptotic cell death. Food Chem. Toxicol. 172, 113564 (2023). https://doi.org/10.1016/j.fct.2022.113564
18. Curtin, N.J.: Targeting the DNA damage response for cancer therapy. Biochem. Soc. Trans. 51(1), 207–221 (2023). https://doi.org/10.1042/bst20220681
19. Juan, L.S., et al.: DNA damage triggers squamous metaplasia in human lung and mammary cells via mitotic checkpoints. Cell Death Discovery 9(1), 1–12 (2023). https://doi.org/10.1038/s41420-023-01330-3
20. Ly, N.P., et al.: Plant-derived nanovesicles: current understanding and applications for cancer therapy. Bioact. Mater. 22, 365–383 (2023). https://doi.org/10.1016/j.bioactmat.2022.10.005
21. Wani, A.K., et al.: Targeting apoptotic pathway of cancer cells with phytochemicals and plant-based nanomaterials. Biomolecules 13(2), 194 (2023). https://doi.org/10.3390/biom13020194

22. Jungwirth, G., et al.: Pharmacological landscape of FDA-approved anticancer drugs reveals sensitivities to ixabepilone, romidepsin, omacetaxine, and carfilzomib in aggressive meningiomas. Clin. Cancer Res. 29(1), 233–243 (2023). https://doi.org/10.1158/1078-0432.ccr-22-2085
23. Sun, W., et al.: Cyanidin-3-O-Glucoside induces the apoptosis of human gastric cancer MKN-45 cells through ROS-mediated signaling pathways. Molecules 28(2), 652 (2023). https://doi.org/10.3390/molecules28020652
24. Liu, X., et al.: Chaetocin induces endoplasmic reticulum stress response and leads to death receptor 5-dependent apoptosis in human non-small cell lung cancer cells. Apoptosis 20(11), 1499–1507 (2015). https://doi.org/10.1007/s10495-015-1167-4
25. Ozyerli-Goknar, E., et al.: The fungal metabolite chaetocin is a sensitizer for pro-apoptotic therapies in glioblastoma. Cell Death Dis. 10(12), 894 (2019). https://doi.org/10.1038/s41419-019-2107-y
26. Wang, H., et al.: ROS/JNK/C-jun pathway is involved in chaetocin induced colorectal cancer cells apoptosis and macrophage phagocytosis enhancement. Front. Pharmacol. 12, 729367 (2021). https://doi.org/10.3389/fphar.2021.729367
27. Jeong, P.S., et al.: Chaetocin improves pig cloning efficiency by enhancing epigenetic reprogramming and autophagic activity. Int. J. Mol. Sci. 21(14), 4836 (2020). https://doi.org/10.3390/ijms21144836
28. Vo, M.C., et al.: Chaetocin enhances dendritic cell function via the induction of heat shock protein and cancer testis antigens in myeloma cells. Oncotarget 8(28), 46047–46056 (2017). https://doi.org/10.18632/oncotarget.17517
29. Jeong, P.-S., et al.: Chaetocin improves pig cloning efficiency by enhancing epigenetic reprogramming and autophagic activity. Int. J. Mol. Sci. 21(14), 4836 (2020). https://doi.org/10.3390/ijms21144836
30. Peng, L., et al.: Preparation of PEG/ZIF-8@ HF drug delivery system for melanoma treatment via oral administration. Drug Deliv. 29(1), 1075–1085 (2022). https://doi.org/10.1080/10717544.2022.2058649
31. Rjiba-Touati, K., et al.: Genotoxic damage and apoptosis in rat glioma (F98) cell line following exposure to bromuconazole. Neurotoxicology 94, 108–116 (2023). https://doi.org/10.1016/j.neuro.2022.11.006
32. Zhang, Q., et al.: TBBPA induces inflammation, apoptosis, and necrosis of skeletal muscle in mice through the ROS/Nrf2/TNF-α signaling pathway. Environ. Pollut. 317, 120745 (2023). https://doi.org/10.1016/j.envpol.2022.120745
33. Ye, J., et al.: Thrombospondin-1 Mimic Peptide PKHB1 Induced Endoplasmic Reticulum Stress-mediated but CD47-independent Apoptosis in Non-small Cell Lung Cancer. Drug Development Research (2023)
34. Gong, M., et al.: A nanodrug combining CD47 and sonodynamic therapy efficiently inhibits osteosarcoma deterioration. J. Contr. Release 355, 68–84 (2023). https://doi.org/10.1016/j.jconrel.2023.01.038
35. Wei, X., et al.: Exosomal lncRNA NEAT1 induces paclitaxel resistance in breast cancer cells and promotes cell migration by targeting miR-133b. Gene 860, 147230 (2023). https://doi.org/10.1016/j.gene.2023.147230
36. Mui, C.W., et al.: Targeting YAP1/TAZ in nonsmall-cell lung carcinoma: from molecular mechanisms to precision medicine. Int. J. Cancer 152(4), 558–571 (2023). https://doi.org/10.1002/ijc.34249
37. Liang, B., et al.: Novel indole-containing hybrids derived from millepachine: synthesis, biological evaluation and antitumor mechanism study. Molecules 28(3), 1481 (2023). https://doi.org/10.3390/molecules28031481

How to cite this article: Zhang, Q., et al.: Natural compound chaetocin induced DNA damage and apoptosis through reactive oxygen species-dependent pathways in A549 lung cancer cells and in vitro evaluations. IET Nanobiotechnol. 17(5), 465–475 (2023). https://doi.org/10.1049/nbt2.12144